Article

Programmable Electrostatic Interactions Expand the Landscape of Dynamic Functional Hydrogels

Sheng-Chen Huang,[†] Xiao-Xia Xia,[†] Ru-Xia Fan, and Zhi-Gang Qian*

Read Online

ACCESS | Metrics & More | Article Recommendations | SI Supporting Information

ABSTRACT: Electrostatic interaction is a promising mechanism to expand the range of physiochemical properties of hydrogel materials. However, the versatility of such materials is still limited because of the difficulties associated with harnessing strong electrostatic interactions for controllable hydrogel formation. Here we report a modular approach for programming interactions between positively charged biopolymers and polyoxometalate (POM) anions to create dynamic hydrogels. Fabrication of diverse hydrogels was achieved simply by soaking primary networks with predispersed chitosan in aqueous solutions of POMs with various nuclearity and charges. This resulted in double network (DN) hydrogels with 2−3 orders of magnitude higher toughness compared with the precedent composite hydrogels. In addition, the dynamic electrostatic interactions endowed the DN hydrogels reversible responsiveness and intriguing capabilities to memorize shapes, to actuate, and to change colors upon exposure to specific external cues, which are challenging to achieve in previous hydrogels. Furthermore, the flexibility of our approach is demonstrated by the use of either physically or chemically cross-linked primary networks, which are composed of synthetic polymers, natural biopolymers, and even genetically engineered protein polymers. Consequently, our facile and modular approach establishes new opportunities in design and fabrication of dynamic functional hydrogels for wide applications.
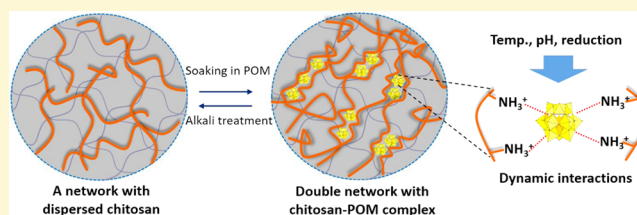
INTRODUCTION

Dynamic functional hydrogels with "smart" behaviors undergo physiochemical changes or shape deformations in response to external stimuli such as temperature,[1−3] pH,[4,5] electricity,[6,7] light,[7,8] or magnetic field.[7,9] Such hydrogels have attracted increasing attention due to their promising applications in soft robotics,[10,11] actuators,[1,10,12,13] and biomaterials.[14−17] The ultimate application of these hydrogels requires a combination of multiple desirable properties such as mechanical properties and smart behaviors.[5,18,19] Extensive efforts have been devoted to synthesizing mechanically robust hydrogels by coupling distinct cross-link mechanisms and networks[19−23] and by introducing nanocomposites and microsphere structures into the hydrogel matrices.[24−27] In a parallel manner, many exciting approaches have been devised to modulate hydrogel responsiveness by the incorporation of stimuli-responsive polymers or cross-linkers within hydrogels.[3−5,27,28] However, achieving robust mechanical properties and multistimuli responsiveness, two highly desirable yet often conflicting properties of hydrogels, remains a great challenge in the field.

Electrostatic interaction is one of the most intriguing dynamic bonds for hydrogel fabrication due to the fast kinetics of complexation reactions[29,30] and responsiveness to multiple external stimuli, including temperature, pH, cations, and anions. For example, the pioneering studies have utilized electrostatic interactions between chains of synthetic polyampholytes[31−33] or oppositely charged polyelectrolytes[30] to form hydrogels with outstanding mechanical properties.
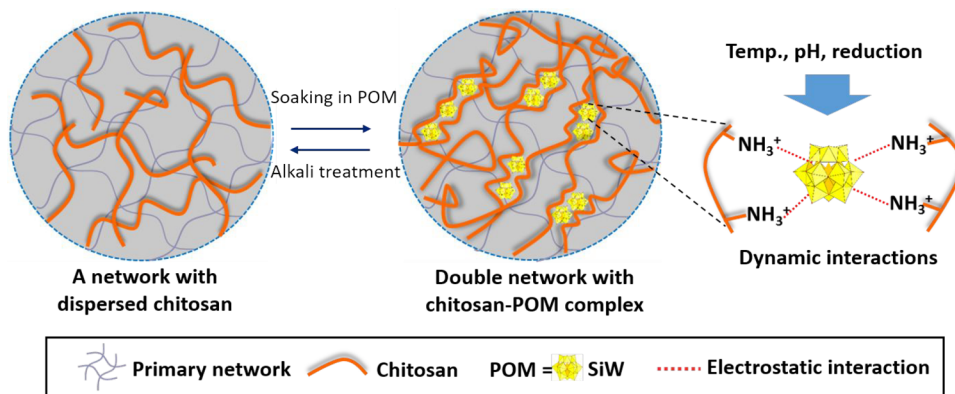
However, the responsiveness of these hydrogels to environmental cues remains unknown. In addition, the types of charged components for hydrogel fabrication are so far still limited, and there is a need to explore new electrostatically interacted pairs of charged components for fabrication of diverse hydrogels with remarkable mechanical properties and dynamic functionalities.

Polyoxometalates (POMs) are a large group of discrete, mostly anionic polynuclear metal-oxo clusters that have well-defined molecular structures and high redox activities with great potential to impart diverse functionalities.[34−37] As a unique type of polyanions, POMs are speculated to form robust hydrogels with polycationic biopolymers by strong electrostatic interactions. The most abundant basic biopolymer, chitosan, has attracted our attention, because it is biodegradable, biocompatible, and readily available in a range of molecular weight (M_w) and degrees of deacetylation.[5,19,21−24,28] In addition, chitosan solutions can be easily prepared for gelation by dissolving chitosan salts in water or by dissolving the chitosan solid in dilute acids. Unfortunately, the
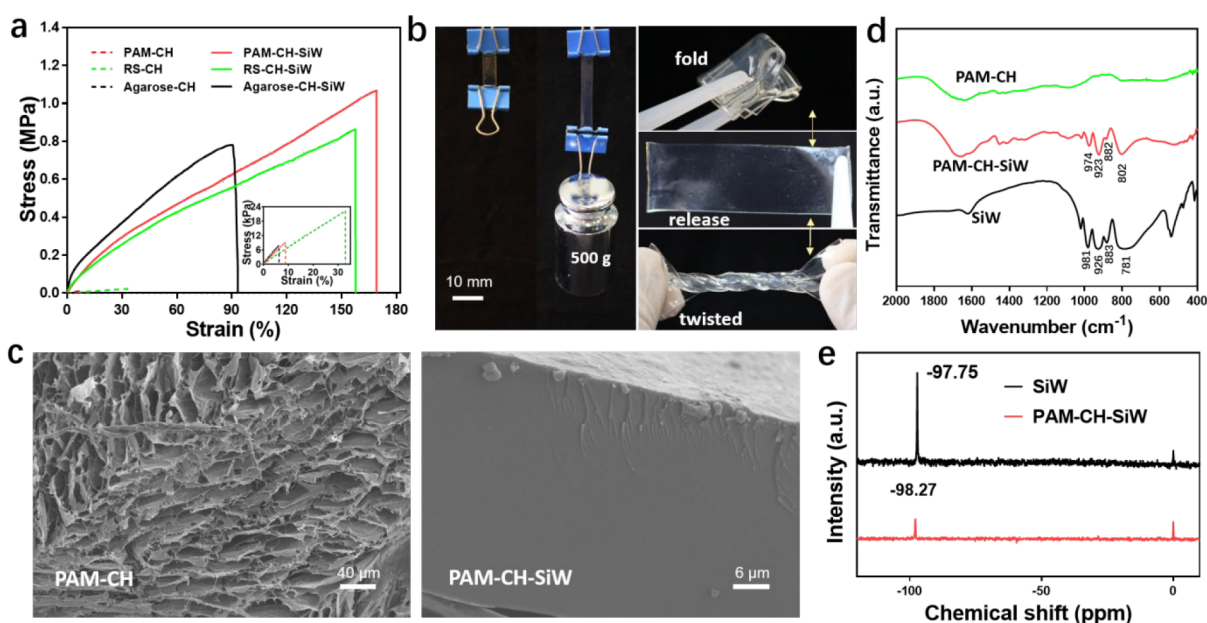
Scheme 1. Programmable Interactions[a]

A network with dispersed chitosan   Double network with chitosan-POM complex   Dynamic interactions

Primary network   Chitosan   POM = SiW   Electrostatic interaction

[a]Programmable interactions between chitosan and POM for the formation of reinforced hydrogels with dynamic behaviors.

Figure 1. (a) Tensile stress–strain curves of the three types of composite and DN hydrogels. (b) Outstanding mechanical performance of the PAM-CH-SiW hydrogels. The hydrogel with a width of 5 mm and thickness of 0.8 mm bore a load of 500 g (left). The hydrogel recovered to its original shape without fracture after it was folded three times or twisted (right). (c) SEM images of the PAM-CH (left) and PAM-CH-SiW (right) hydrogels. (d) FTIR spectra of SiW, PAM-CH composite, and PAM-CH-SiW DN hydrogels in the range of 2000−400 cm^{-1}. (e) ^{183}W NMR spectra of SiW alone and lyophilized PAM-CH-SiW hydrogel dissolved in DMSO-d_6. The signal at 0 ppm is the reference (2 M Na$_2$WO$_4$ aqueous solution in D$_2$O).

fast complexation between chitosan and POM solutions (Figure S1) prevents the formation of bulk hydrogels.

To overcome the obstacle for controllable hydrogel formation, here we propose a new approach by soaking a primary network with predispersed chitosan into POM solutions to form double network (DN) hydrogels (Scheme 1). This approach has at least three merits, as follows. First, facile soaking allows free diffusion of the nanometer-sized POM anions into the existing primary network for controllable cross-linking with positively charged chitosan. Second, the electrostatic interaction complements rather than restricts the type of primary network, either chemically or physically cross-linked. Third, the modular and versatile strategy could not only confer sacrificial bonds to strengthen and toughen hydrogels but also incorporate stimuli-responsive cross-linkers to impart dynamic properties.

■ RESULTS AND DISCUSSION

To demonstrate the modular feature of our approach, chitosan hydrochloride (CH) of low molecular weight (30 kDa) was first chosen and mixed with building blocks of distinct primary networks. Here, two chemically cross-linked matrices of either synthetic polyacrylamide (PAM) or genetically engineered resilin-silk (RS) copolymer[38] and a physically cross-linked matrix of natural biopolymer agarose were shown as model primary networks. These composite hydrogels, labeled as PAM-CH, RS-CH, and agarose-CH, were then soaked into solution of a Keggin-type POM, silicotungstic acid (SiW). SiW is a particularly unique polyanionic nanocluster (1.00 × 1.00 × 1.00 nm^3) with a rigid framework, well-defined topology, high ionization propensity in water, single size distribution, and electrochromism,[39] and thus was chosen as a cross-linker to form quadrivalent electrostatic interactions with positively charged CH. The resulting double network hydrogels all

Table 1. Tensile Mechanical Properties of Various Hydrogels

hydrogel type	strength (kPa)	strain at break (%)	elastic modulus (MPa)	toughness (kJ m^{-3})
composite hydrogel^a				
PAM-3% CH	9.5 ± 0.4	8.9 ± 1.7	0.12 ± 0.04	0.42 ± 0.11
PAM-3% CH$_{MMw}$	12.0 ± 0.6	12.0 ± 1.5	0.15 ± 0.02	0.75 ± 0.15
RS-3% CH	24.0 ± 3.2	32.9 ± 4.5	0.09 ± 0.01	3.76 ± 0.48
agarose-2% CH	8.1 ± 0.4	6.3 ± 0.2	0.16 ± 0.01	0.27 ± 0.03
double network hydrogel^b				
PAM-3% CH-SiW	1054.8 ± 153.3	178.8 ± 18.5	1.88 ± 0.12	1094.3 ± 78.5
PAM-3% CH-PMo	540.6 ± 67.7	138.7 ± 19.2	3.01 ± 0.44	692.3 ± 57.0
PAM-3% CH-PW	1180.5 ± 114.8	113.9 ± 12.2	2.29 ± 0.24	746.8 ± 53.1
PAM-3% CH$_{MMw}$-SiW	3272.7 ± 224.0	234.3 ± 20.8	3.97 ± 0.29	4090.9 ± 121.6
RS-3% CH-SiW	861.8 ± 92.3	159.6 ± 16.5	2.37 ± 0.45	774.8 ± 34.2
agarose-2% CH-SiW	812.8 ± 53.0	93.7 ± 8.5	5.28 ± 0.88	450.9 ± 28.8

^{a}CH and CH$_{MMw}$ stand for the low (30 kDa) and medium (200 kDa) molecular weight chitosan hydrochloride used for hydrogel fabrication. ^{b}Abbreviations for diverse POMs: SiW, H$_4$SiW$_{12}$O$_{40}$; PMo, H$_3$PMo$_{12}$O$_{40}$, and PW, H$_3$PW$_{12}$O$_{40}$.
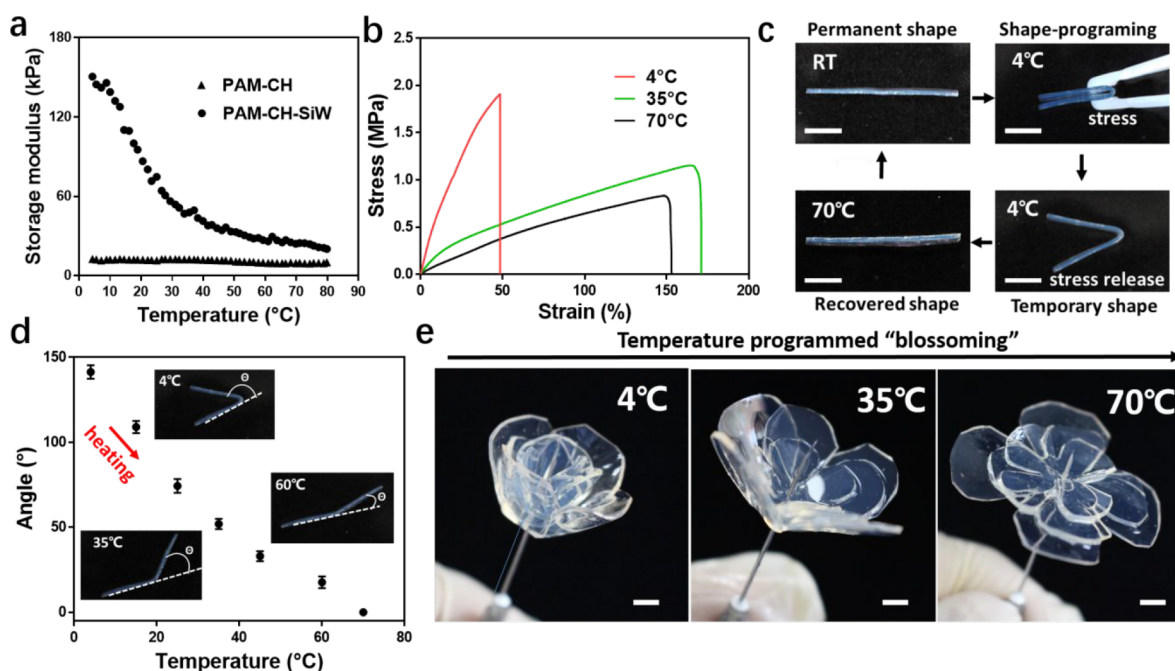

Figure 2. (a) The storage modulus of the PAM-CH-SiW and PAM-CH hydrogels as a function of temperature at a heating rate of 2 °C min^{-1} in rheological tests. (b) Tensile stress−strain curves of the PAM-CH-SiW hydrogels at various temperatures. (c) Shapeshifting cycle of the PAM-CH-SiW hydrogel: an initial rodlike sample is bent to a hairpin at 25 °C by external stress, and the deformed temporary shape is fixed upon cooling at 4 °C. When heated to 70 °C, the original, rodlike shape is recovered. Note that the hydrogel does not have a volume change with temperature. (d) Hairpin angle (θ) was monitored for the shape-programmed hydrogel during the heating-triggered shape-memory process. The data represent the average of three replicates, and error bars correspond to the standard deviations. (e) An artifact bud "blooming" captured during the heating process. Scale bar, 5 mm.

displayed greatly improved mechanical properties over the corresponding composite hydrogels (Figure 1a). For example, the PAM-CH-SiW DN hydrogel exhibited a fracture strength and fracture energy of ~1.05 MPa and 1.09 MJ m^{-3}, respectively, which were 111- and 2605-fold higher than those of the preceding composite gel. Furthermore, soaking the PAM-CH hydrogels in solutions of POMs with varying nuclearity and charges also resulted in DN hydrogels with reinforced mechanical properties (Figure S2a). When CH of medium molecular weight (200 kDa) was used in hydrogel fabrication, the resulting DN gels showed even better mechanical properties (Figure S2b), with an elastic modulus, fracture strength, and fracture energy of 3.97 MPa, 3.27 MPa, and 4.09 MJ m^{-3}, respectively (Table 1). Notably, the

reinforcing effects on the mechanical properties of the DN hydrogels correlated positively with the concentrations of CH dispersed in the primary networks (Figure S3 and Table S1). Taken together, these results indicate that a wide variety of tough hydrogels could be fabricated by varying the type of POMs, molecular weight, and concentration of CH, and the choice of primary networks.

As vividly displayed in Figure 1b, a ribbon of the pristine PAM-CH-SiW hydrogel with a 4 mm^2 cross section could bear a weight of 500 g, showing an appreciably high loading ability. In addition, the gel could be twisted into a helical shape or folded three times and recover to its original shape without fracture, indicating its good toughness and shape self-recoverability. When the chemically cross-linked primary
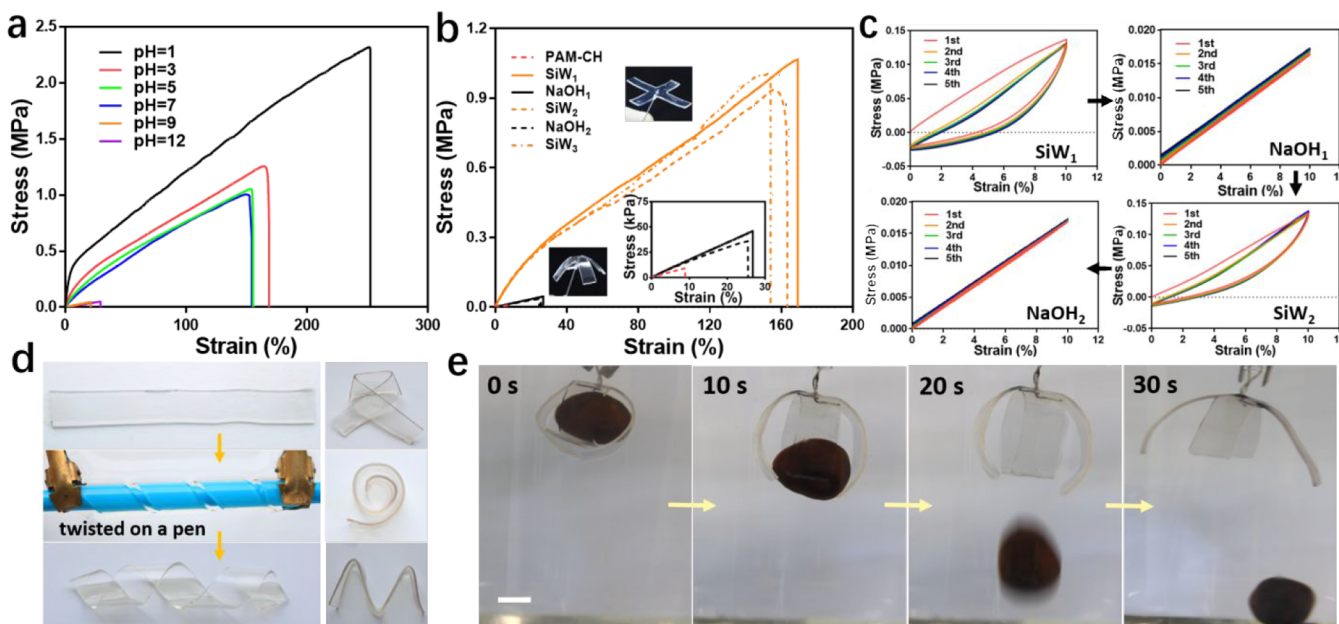
Figure 3. (a) Tensile stress—strain curves of the PAM-CH-SiW hydrogels conditioned over a wide pH range from 1 to 12. (b) The PAM-CH-SiW hydrogels exhibited switchable tensile properties upon alternating treatments with 0.1 M NaOH and 0.17 M SiW. The PAM-CH composite hydrogel was soaked in the SiW solution to make the DN hydrogel (named SiW_1), which was treated with NaOH and SiW in an alternating manner. (c) Five successive loading—unloading cycles of a PAM-CH-SiW hydrogel upon alternating treatments with NaOH and SiW as described in (b). The hydrogel was tensile tested to 10% strain after each treatment. (d) Molding of the PAM-CH-SiW DN hydrogel: a hydrogel bar is twisted on a pen and soaked in the SiW solution to program its shape into a helix (left). Similarly, the hydrogel bar can be programmed into other arbitrary shapes such as a tie, a spiral, and an "M" (right). (e) A claw-shaped PAM-CH-SiW DN hydrogel released a 5 g brown object into a basic solution (0.1 M NaOH). Scale bar, 10 mm.

network was replaced with the physical network of agarose, the resulting DN hydrogel was endowed with an intriguing shape moldable property, as demonstrated by the complex, arbitrary shapes such as hydrogel "plane" and "crane" (Figure S4). Therefore, the integration of CH-POM ionic networks not only toughened the hydrogels but also endowed shape-morphing properties. Scanning electron microscopy (SEM) revealed the formation of compact and dense microstructures due to the integration of the ionic networks (Figure 1c and Figure S5), which coincided well with the reinforced mechanical properties for the DN hydrogels. Furthermore, the reversible ionic networks endowed the hydrogels with good self-recovery ability based on tensile tests on the stretched hydrogel samples after different relaxing times (Figure S6).

Next, the Fourier-transform infrared spectroscopy (FTIR) spectra of the DN hydrogels were analyzed. As shown in Figure 1d, the FTIR spectra of the PAM-CH-SiW hydrogel present the characteristic vibrations bands of SiW at 974, 923, 882, and 802 cm^{-1}, whereas such bands were not observed for the composite hydrogels. Notably, the above characteristic bands were slightly shifted when compared with those of the parent SiW. This was attributed to modification of the SiW microenvironments as a result of electrostatic interactions with protonated amino groups of CH.[37,40] Similar results were observed for the RS-CH-SiW and agarose-CH-SiW hydrogels (Figure S7), demonstrating the formation of electrostatic interactions involving SiW in the DN hydrogels tested.

Furthermore, ^{183}W nuclear magnetic resonance (NMR) spectroscopy was performed to evaluate integrity of SiW in the DN hydrogels. As shown in Figure 1e and Figure S8, deuterated dimethyl sulfoxide (DMSO-d_6) solutions of all the lyophilized DN hydrogels showed the ^{183}W NMR chemical shifts characteristic of SiW alone in the same solvent,[37,40]

indicating that the topological structure of SiW was well-retained within the DN hydrogels. In addition, elemental analysis of the lyophilized PAM-CH-SiW hydrogel revealed a weight percentage of 1.46 ± 0.34 wt % for silicon, further demonstrating the existence of SiW in the hydrogel matrix.

Having characterized the DN hydrogels, we then explored whether the dynamic electrostatic interactions could impart temperature responsiveness to the hydrogels. As a typical example, the PAM-CH-SiW hydrogel was chosen for rheological characterization over a broad temperature range. The temperature sweep analysis, which monitors evolution of modulus with increasing temperature, revealed that the hydrogel stiffness decreased sharply at the initial stage and then declined slowly after 35 °C (Figure 2a). In contrast, the PAM-CH gel without the CH-SiW ionic network maintained nearly constant modulus, which demonstrates that the electrostatic interaction within the CH-SiW network is sensitive to temperature. The temperature responsiveness of the DN hydrogels was also observed in uniaxial tensile tests (Figure 2b). For example, the elastic modulus of the PAM-CH-SiW hydrogel was 7.53 MPa at the chilling temperature of 4 °C. As the temperature was increased to 35 °C, the DN hydrogel was substantially softened, with elastic modulus at 1.82 MPa, and became at least 3 times more extensible. These results indicate the huge changes in tensile mechanical properties of the DN hydrogels even in the narrow temperature range of physiological relevance.

On the basis of the above results, we further explored whether the DN hydrogels could be thermally programmed for use as shape memory materials. In principle, when the deformed DN hydrogels are fixed at lower temperatures, the electrostatic interactions will become strong enough to temporarily lock-in the deformed shape, and the covalent
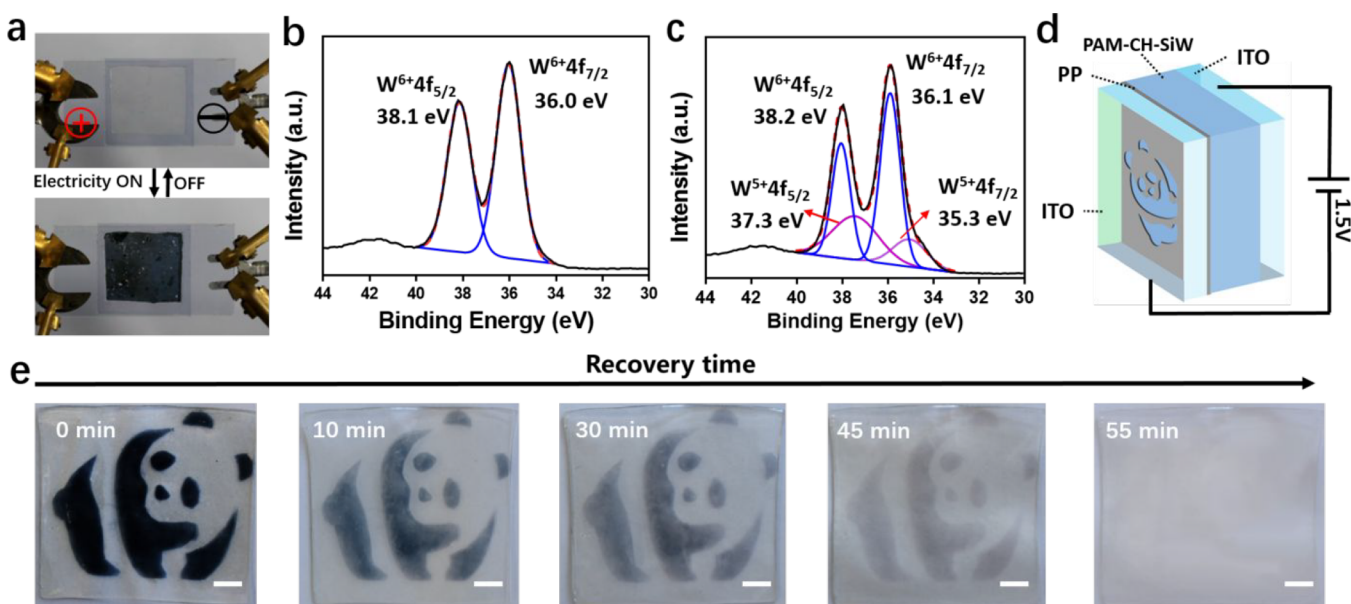
Figure 4. (a) Photographs of the PAM-CH-SiW hydrogel placed on an ITO-coated glass slide, exhibiting reversible electrochromic behavior. XPS spectra of the hydrogel before (b) and after (c) the electrochemical reduction. (d) 3D schematic diagram of the PAM-CH-SiW hydrogel-based printer device, in which a PP insulation film with a carved hollow pattern was closely adhered to the hydrogel and then placed between two ITO-coated glass plates. (e) Images of the printed "panda" pattern captured at different times during the decoloration process, which was due to oxidation of W^{5+} (deep blue) into W^{6+} (colorless) by atmospheric oxygen. Scale bar, 5 mm.

cross-links of the primary networks store the elastic energy. With an increase in temperature, the "locks" will gradually dismiss, and the covalent cross-links will release the energy to drive shape recovery. To test the hypothesis, we designed a shape programming and recovery process for the PAM-CH-SiW hydrogel (Figure 2c). A rodlike hydrogel (permanent shape) was folded along the horizontal axis at room temperature to a hairpin shape. The hairpin under external stress was fixed at 4 °C for 10 min to obtain a temporary shape. Upon removal of the external stress, the hairpin sample partially recovered and then maintained a temporary shape at the chilling temperature. When subsequently heated to 70 °C, the hairpin unfolded and recovered to its original straight shape instantaneously. In addition, the recovered sample could be immediately shape-morphed in another shape memory cycle, and the reversible shape memory transitions could be repeated for at least 30 times. More interestingly, the shape-programmed rodlike hydrogel displayed a stepwise recovery process as a function of temperature during the heating process (Figures S9 and S10). To describe the shape morphing process quantitatively, we recorded angle θ, which represented the position of each recovered shape relative to the original permanent shape of the hydrogel. Figure 2d displays the nonlinear relationship between the angle θ and the temperature during the heating process. The angle θ was ~142° for the programmed hydrogel at 4 °C and gradually decreased to ~51° at 35 °C. Upon further heating to 70 °C, the sample almost completely restored its original shape ($\theta \approx 0°$). Furthermore, the shape programming and recovery process was reproducible for at least 20 cycles (Figure S11), and the intriguing shape memory effect motivated us to create an artificial three-dimensional (3D) hydrogel "flower" with thermally triggered "blooming" (Figure 2e and Movie S1). Notably, the PAM-CH-SiW hydrogels were responsive to temperature changes and supportive of shape morphing in the narrow temperature range of physiological relevance, and this

unique feature, to the best of our knowledge, has not been previously reported for gels with ionic cross-linking.

Intuitively, pH strongly affects protonation of the amino groups (pK_a 6.3[41]) in the CH chain, and the number of ionic cross-links in the DN hydrogels correlates directly to the amount of protonated amino groups. Therefore, we examined pH responsiveness of the DN hydrogels over a wide pH range of 1−12. To this end, we performed tensile tests for the PAM-CH-SiW hydrogels (Figure 3a). The hydrogels tended to display superior mechanical performance with a decrease in pH, because increasing acidity favored protonation of the amino groups for ionic cross-linking with the SiW anions. On the one hand, notably, the hydrogel at pH 1 showed remarkable mechanical properties (elastic modulus: 7.95 MPa; tensile fracture stress: 2.32 MPa; tensile fracture strain: 253%). On the other hand, the hydrogel mechanical properties were unaffected under weakly acidic (pH 5) to neutral pH, possibly due to the proportion of protonated amino groups being comparable at pH levels close to the pK_a. When the pH was further increased to 9 and higher levels, dramatic decreases in mechanical properties were observed. According to Jürgensen and Moffat,[42] the extent of SiW decomposition was only 25% at a pH of 8.9 in aqueous solution, and it increased to 100% at pH 11.0. To explore the integrity of SiW in the PAM-CH-SiW hydrogels, we monitored the FTIR spectra of the gels conditioned at pH values of 7 and 9, respectively. Interestingly, characteristic FTIR spectra of SiW were observed for the gels at both pH conditions, whereas the chitosan-SiW electrostatic interactions collapsed at pH 9 (Figure S12). Therefore, the inferior hydrogel mechanical properties at pH 9 were due to loss of the ionic cross-links resulting from deprotonation of the amino groups in the CH chains and partial decomposition of the SiW clusters in the gel.

Owing to the pH-responsive cross-linking mechanism, the mechanical properties of the hydrogels might be reversibly switched between tough and weak. To demonstrate this,

tensile tests were performed for the hydrogel samples alternately immersed in SiW and NaOH solutions (Figure 3b and Figure S13). As expected, the PAM-CH-SiW hydrogels could repeatedly switch between tough (by SiW treatment) and weak (by NaOH treatment). Notably, the NaOH-treated hydrogels exhibited slightly improved mechanical performance compared with the initial composite hydrogels due to the self-assembly of the deprotonated CH through hydrogen bonding and hydrophobic interactions. The inserted photographs in Figure 3b vividly showed that the SiW-treated hydrogel was tough enough to self-support its weight in the air without noticeable deformation, whereas the NaOH-treated hydrogel was too weak to self-support. Interestingly, the two morphological states could repeatedly switch by the above-mentioned treatments. To characterize mechanical behaviors of the treated hydrogels, successive loading−unloading tests were performed for individual hydrogels upon alternating treatments with SiW and NaOH. As illustrated in Figure 3c, the SiW-treated hydrogel exhibited typical viscoelastic behavior with significant hysteresis loops, indicating its good energy dissipation capacity due to the reconfigurable "sacrificial bonds" of CH-SiW in tensile tests. In the absence of the sacrificial bonds, the NaOH-treated hydrogel switched back to being elastic and displayed unobservable hysteresis. Similar tests were performed for the RS-CH-SiW and agarose-CH-SiW hydrogels, also revealing a switch in energy-dissipating capacity (Figure S14).

The above switchable properties motivated us to remold the hydrogels into various 3D structures. As shown in Figure 3d, the NaOH-treated PAM-CH-SiW hydrogel, which is soft and withstands a great deal of bending, was twisted on a pen and then immersed in SiW solution for 1 h. The newly formed CH-SiW interactions were sufficiently strong to fix the polymer chains enabling the hydrogel with a helical shape. When the above molded hydrogel was soaked in NaOH solution for 1 h, the shape gradually returned to its initial state. In a similar manner, the same piece of the hydrogel could be remolded into various arbitrary shapes including a "bow tie", a spiral and "letter M". This remoldable and responsive property indicated that the hydrogel can be potentially used as actuators. Figure 3e illustrates a prototype of a claw molded from the PAM-CH-SiW hydrogel. The claw with an enclosed object could release the object within 10 s when immersed in a basic solution due to the disintegration of the CH-SiW electrostatic interactions. In addition, the above cycle of claw molding and object release could be performed repeatedly at least 30 times, indicating desirable reusability of the hydrogel actuator.

Diverse POMs are amenable to reduction, and reduced POMs usually have the same general atomic structure as the oxidized POMs.[35] Inspired by the redox activity of POMs, we then explored whether the DN hydrogels were responsive to electrochemical reduction (Figure 4a). When the PAM-CH-SiW gel with a thickness of 0.8 mm was placed between two electrically conductive indium tin oxide (ITO)-coated glass plates with applied voltage, the transparent hydrogel changed within 5 s from colorless to deep blue (Movie S2), a characteristic color of reduced POMs.[35] More interestingly, the hydrogel switched to being colorless and transparent after the voltage was turned off for 55 min (Figure S15), showing a reversible electrochromic behavior. Notably, the electro-chromic inking kinetics is fast and comparable to previous POM-based electrochromic devices,[43] whereas the bleaching kinetics is ~1 order of magnitude slower. The slow kinetics of

bleaching might be due to the low capability of atmospheric oxygen in oxidizing W^{5+} to W^{6+} (see below) and/or to the oxygen transport processes. However, the detailed mechanisms remain to be explored.

To explore the chemical mechanism of electrochromics, X-ray photoelectron spectroscopy (XPS) was employed to analyze surface composition of the PAM-CH-SiW hydrogel before and after electrochemical reduction. As shown in Figure 4b, the pristine hydrogel showed XPS peaks at 38.1 and 36.0 eV, which are attributed to the electron binding energy of W^{6+} $4f_{5/2}$ and W^{6+} $4f_{7/2}$, respectively.[37] In contrast, the reduced hydrogel exhibited two deconvoluted peaks at 37.3 and 35.3 eV (Figure 4c), which were assigned to the binding energy of W^{5+} $4f_{5/2}$ and W^{5+} $4f_{7/2}$, respectively.[37] These two emerging peaks can be distinctly attributed to the $W^{6+} \rightarrow W^{5+}$ intervalence charge transfer, indicating the formation of reduced SiW in the electrochromic process. During the autonomous decoloration process, molecular oxygen in the atmosphere is reduced to oxidize W^{5+} into W^{6+} again.

Benefiting from the reversible electrochromic property, the DN hydrogels might be used as ink-free rewritable materials. As a proof-of-concept example, a simple ink-free printer was fabricated that can "print" designed patterns on the hydrogel. Figure 4d shows a 3D schematic representation of the printer, in which a polypropylene (PP) insulation film with a carved hollow pattern is closely adhered to the PAM-CH-SiW hydrogel and then placed between two ITO-coated glass plates. For example, the PP film with a hollowed panda pattern (Figure S16) permitted exposure of the hydrogel to electricity only through the hollows of the PP film. The deep blue pattern of a "panda" appeared distinctly on the gel after applying voltage and then faded gradually in the air and completely recovered to its original state in 55 min (Figure 4e). Notably, the recovered hydrogel can be "printed" again with such coloration-decoloration cycle for at least 15 times. By using electricity as "printing ink", any text and pattern, in principle, can be printed on this hydrogel and erased arbitrarily. As a new member of the family of electrochromic materials, the POM-harboring hydrogels provide an alternative for rewritable pattern display.

■ CONCLUSION

In summary, we have established a modular approach for programming electrostatic interactions between the positively charged chitosan and POM anions to create a new series of dynamic hydrogels. Our approach is flexible to tune hydrogels with a broad range of mechanical properties, simply by orthogonally composing the gelation system. This can be facilely achieved by adjusting the molecular weight of chitosan, the primary network for chitosan predispersion, and POM solutions for soaking. With integration of the strong electro-static interactions, hydrogels with outstanding stiffness, strength, and toughness have been fabricated to fulfill the mechanical needs for actuation. Intriguingly, the dynamic electrostatic interactions endow the mechanically robust hydrogels responsiveness to diverse stimuli, thus offering two features that are highly desirable and seldom achieved in previously reported soft materials. Of particular interest, the hydrogels are responsive to various easily applicable stimuli including temperature, pH, and reduction, in a reversible and programmable manner. This feature has enabled fabrication of the hydrogels into multiple arbitrary 3D objects to morph shapes, to actuate and display color changes with appreciable

repeatability and durability. Combined with the recent developments in 3D printing of complex shapes,[44] our gelation system and the resulting dynamic hydrogels could significantly expand the technical potential for applications in soft robotics, rewritable display, and electricity sensor. Nonetheless, because of the unspecific cytotoxicity of POMs against tumor and normal cells,[45] the biocompatibility of the POM-containing hydrogels needs to be carefully evaluated for possible biomedical applications.

■ MATERIALS AND METHODS

Chemicals and Materials. A 30 wt % solution of acrylamide/ N,N'-methylenebis(acrylamide) (29:1), agarose, and ammonium persulfate (APS) were obtained from Sangon Biotech, Tsingke Biotech, and Amresco, respectively. CH of low M_w (30 kDa, >90% deacetylated) and its medium M_w counterpart (CH$_{MMw}$; 200 kDa, 80−95% deacetylated) were purchased from Karma Chem and Maokang Biotechnology Co., Ltd., respectively. Phosphomolybdic acid hydrate, phosphotungstic acid hydrate, and tungstosilicic acid hydrate were obtained from Nine-Ding Chemical, Macklin Biochemical, and Aladdin Biochemical, respectively. Tris(2,2′-bipyridyl)-dichlororuthenium(II) hexahydrate was obtained from Sigma. The RS protein polymer (49.2 kDa) was biosynthesized as described in our previous study.[38] All other chemicals and reagents were of analytical purity and used without further purification.

Preparation of Composite Hydrogels. Three types of composite hydrogels were prepared. In one experiment, powders of CH were suspended in the 30 wt % acrylamide/N,N'-methylenebis-(acrylamide) (AM/MBA) solution and stirred overnight at room temperature. Following the addition of APS and degassing with nitrogen stream, the solutions containing 10 wt % AM/MBA, 0.1 wt % APS, and 3 wt % CH (unless specified otherwise) were poured into glass molds and incubated at 60 °C for 4 h to yield the as-prepared PAM-CH composite hydrogels. Similarly, PAM-CH$_{MMw}$ composite gels were prepared by dispersing CH$_{MMw}$ in the pregelation solutions. In another experiment, CH, RS protein, [Ru(bpy)$_3$]$^{2+}$, and APS were dissolved in deionized water at final concentrations of 3 wt % (unless specified otherwise), 10 wt %, 2 mM, and 10 mM, respectively. The solutions were then transferred into bar molds and irradiated for 4 min with a 200 W white light source. The third type of composite hydrogels was fabricated by pouring hot, aqueous solutions of 2 wt % agarose and 0.5−2 wt % CH into glass molds to cool for 1 h at room temperature.

Preparation of DN Hydrogels. The above three types of composite hydrogels were immersed in 0.17 M aqueous solution of the indicated POM for 1 h (unless specified otherwise) at room temperature. For removal of the dissociative POM clusters, the hydrogels were first briefly rinsed with deionized water and then soaked in fresh water overnight. Afterward, the hydrogels were taken out and gently blotted with filter papers to remove surface liquids. The as-prepared DN hydrogels were then tested and characterized as described below. In another experiment, the PAM-CH composite hydrogels were soaked in the SiW solution for varying periods of time (5−720 min), similarly washed, and tensile tested, which revealed that 45 min of soaking was sufficient to reach full loading with the POM (Figure S17).

Mechanical Property Tests. Tensile tests were performed on an Instron 5944 testing machine with a 10 N load cell (Instron Corporation). Briefly, rectangular hydrogel samples were coated with dimethylsilicone oil to minimize moisture evaporation and tested at 25 °C and 60% relative humidity in air. For the temperature-dependent tensile tests, the specimens were placed in a water bath at 4, 35, or 70 °C. The deformation rate of nominal tensile tests to rupture was set at 10 mm min^{-1}. Cyclic loading−unloading tensile tests were performed at 25 °C and a deformation rate of 2 mm min^{-1} with five continuously repeated cycles. For rheological measurements, a stress-controlled AR-G2 rheometer with a 40 mm parallel-plate configuration (TA Instruments) was used. Samples with a thickness of

0.8 mm and a diameter of 40 mm were loaded onto the precooled bottom plate, with hydrogenated silicone added between the top and bottom plates to minimize hydrogel dehydration. The temperature sweeps from 4 to 80 °C with a heating rate of 2 °C min^{-1} were then performed at a frequency of 1 Hz and a strain 1%, which was within the linear viscoelastic regime.

Electrochromic test. The electrochromic experiments for the as-prepared DN hydrogels were performed on a CHI760E electrochemical workstation (Chenhua Instrumental Co.). The hydrogel samples were individually loaded on the ITO-coated glass. Then, a second ITO-coated glass electrode with a layer of insulated PP mask was placed on the gel. Photographs and videos were taken for the gels using a Canon EOS 700D camera (Canon).

Characterization of Hydrogels. FTIR analyses of lyophilized hydrogels were performed on a Nicolet 6700 spectrometer (Thermo Fisher Scientific Inc.) equipped with a deuterated triglycine sulfate detector. ^{183}W NMR spectra were acquired on an Avance III 400 MHz spectrometer (Bruker), with 2 M Na$_2$WO$_4$ solution in D$_2$O as an external reference. Prior to analyses, lyophilized hydrogels and tungstosilicic acid hydrate were dissolved in DMSO-d_6, respectively. SEM images were acquired on a Hitachi S-3400N scanning electron microscope. To prepare the specimens, lyophilized hydrogels were coated with gold using a Leica EM SCD050 sputtering device with a water-cooled sputter head (Leica Microsystems GmbH). XPS spectra were acquired on an AXIS Ultra DLD spectrometer (Kratos). The hydrogels before and after electrochemical reduction were frozen in liquid nitrogen for 15 min and lyophilized under vacuum for XPS analyses. All the peaks were charge-corrected using the binding energy of C (1s) at 284.6 eV as the reference point. The OriginPro v9.2 software (OriginLab Corp.) was used for baseline correction and subsequent iterative curve fitting of the spectra using Gaussian algorithm with R^2 more than 0.998, in which the second derivatives of the spectra were used for peak positioning guidance. For elemental analysis, the hydrogels were lyophilized, ground into powders, and loaded into an iCAP 6300 inductively coupled plasma optical emission spectrometer (Thermo Fisher Scientific). The deep blue intensity of the PAM-CH-SiW hydrogels in electrochromic processes was monitored by measuring absorbance at 700 nm using a Lamda 950 UV−vis−NIR (NIR = near-infrared) spectrophotometer (PerkinElmer).

■ ASSOCIATED CONTENT

ⓢ Supporting Information

The Supporting Information is available free of charge at https://pubs.acs.org/doi/10.1021/acs.chemmater.9b04726.

> Tensile mechanical properties of hydrogels, formation of thin films at the interface of chitosan and POM solutions, tensile tests for the DN hydrogels with varying types of POMs, molecular weight and concentration of chitosan, photographs of the agarose-CH-SiW DN hydrogel molded into different shapes, SEM images of various hydrogels, self-recovery behavior of the PAM-CH-SiW DN hydrogel, FTIR and ^{183}W NMR spectra of various hydrogels, images of rodlike DN hydrogels captured at different temperatures in the temperature-triggered shape memory cycle, gel hairpin angle in different cycles of the heating-triggered shape memory process, FTIR spectra of the DN hydrogels conditioned at pH 7 and 9, tensile tests and successive loading−unloading cycles for the hydrogels with alternating treatments of SiW and NaOH, gel color change during the "inking" and bleaching processes, photograph of the PP insulation film with a carved hollow "panda" pattern, tensile tests for the DN hydrogels with varying time of soaking in the SiW solution (PDF)

Illustration of an artificial 3D hydrogel "flower" with thermally triggered "blooming" (MP4)

Electrochromic behavior of the PAM-CH-SiW DN hydrogel (MP4)

■ AUTHOR INFORMATION

Corresponding Author

Zhi-Gang Qian − *State Key Laboratory of Microbial Metabolism, Joint International Research Laboratory of Metabolic & Developmental Sciences, and School of Life Sciences and Biotechnology, Shanghai Jiao Tong University, Shanghai 200240, People's Republic of China;* ● orcid.org/0000-0002-0133-0605; Email: zgqian@sjtu.edu.cn

Authors

Sheng-Chen Huang − *State Key Laboratory of Microbial Metabolism, Joint International Research Laboratory of Metabolic & Developmental Sciences, and School of Life Sciences and Biotechnology, Shanghai Jiao Tong University, Shanghai 200240, People's Republic of China*

Xiao-Xia Xia − *State Key Laboratory of Microbial Metabolism, Joint International Research Laboratory of Metabolic & Developmental Sciences, and School of Life Sciences and Biotechnology, Shanghai Jiao Tong University, Shanghai 200240, People's Republic of China;* ● orcid.org/0000-0001-8375-1616

Ru-Xia Fan − *State Key Laboratory of Microbial Metabolism, Joint International Research Laboratory of Metabolic & Developmental Sciences, and School of Life Sciences and Biotechnology, Shanghai Jiao Tong University, Shanghai 200240, People's Republic of China*

Complete contact information is available at:
https://pubs.acs.org/10.1021/acs.chemmater.9b04726

Author Contributions

[†]These authors contributed equally to this work (S.-C.H. and X.-X.X.).

Notes

The authors declare no competing financial interest.

■ ACKNOWLEDGMENTS

■ REFERENCES

(1) Kim, Y. S.; Liu, M.; Ishida, Y.; Ebina, Y.; Osada, M.; Sasaki, T.; Hikima, T.; Takata, M.; Aida, T. Thermoresponsive Actuation Enabled by Permittivity Switching in an Electrostatically Anisotropic Hydrogel. *Nat. Mater.* **2015**, *14*, 1002−1007.

(2) Deng, Z.; Guo, Y.; Zhao, X.; Ma, P. X.; Guo, B. Multifunctional Stimuli-Responsive Hydrogels with Self-Healing, High Conductivity, and Rapid Recovery through Host−Guest Interactions. *Chem. Mater.* **2018**, *30*, 1729−1742.

(3) Hu, X. B.; Zhang, D. X.; Sheiko, S. S. Cooling-Triggered Shapeshifting Hydrogels with Multi-Shape Memory Performance. *Adv. Mater.* **2018**, *30*, 1707461.

(4) Tsai, C. C.; Payne, G. F.; Shen, J. Exploring pH-Responsive, Switchable Crosslinking Mechanisms for Programming Reconfigurable Hydrogels Based on Aminopolysaccharides. *Chem. Mater.* **2018**, *30*, 8597−8605.

(5) He, H.; Cao, X.; Dong, H.; Ma, T.; Payne, G. F. Reversible Programing of Soft Matter with Reconfigurable Mechanical Properties. *Adv. Funct. Mater.* **2017**, *27*, 1605665.

(6) Xue, B.; Qin, M.; Wang, T.; Wu, J.; Luo, D.; Jiang, Q.; Li, Y.; Cao, Y.; Wang, W. Electrically Controllable Actuators Based on Supramolecular Peptide Hydrogels. *Adv. Funct. Mater.* **2016**, *26*, 9053−9062.

(7) Merino, S.; Martín, C.; Kostarelos, K.; Prato, M.; Vázquez, E. Nanocomposite Hydrogels: 3D Polymer−Nanoparticle Synergies for On-Demand Drug Delivery. *ACS Nano* **2015**, *9*, 4686−4697.

(8) Li, L.; Scheiger, J. M.; Levkin, P. A. Design and Applications of Photoresponsive Hydrogels. *Adv. Mater.* **2019**, *31*, 1807333.

(9) Li, Y.; Huang, G.; Zhang, X.; Li, B.; Chen, Y.; Lu, T.; Lu, T. J.; Xu, F. Magnetic Hydrogels and Their Potential Biomedical Applications. *Adv. Funct. Mater.* **2013**, *23*, 660−672.

(10) Yuk, H.; Lin, S.; Ma, C.; Takaffoli, M.; Fang, N. X.; Zhao, X. Hydraulic Hydrogel Actuators and Robots Optically and Sonically Camouflaged in Water. *Nat. Commun.* **2017**, *8*, 14230.

(11) Jung, D.; Lee, K. M.; Tojo, T.; Oh, Y.; Yoon, H.; Kim, H. Dual Cross-Linked Hydrogels That Undergo Structural Transformation via Selective Triggered Depolymerization. *Chem. Mater.* **2019**, *31*, 6249−6256.

(12) Lin, H.; Ma, S.; Yu, B.; Pei, X.; Cai, M.; Zheng, Z.; Zhou, F.; Liu, W. Simultaneous Surface Covalent Bonding and Radical Polymerization for Constructing Robust Soft Actuators with Fast Underwater Response. *Chem. Mater.* **2019**, *31*, 9504.

(13) Le, X.; Lu, W.; Zhang, J.; Chen, T. Recent Progress in Biomimetic Anisotropic Hydrogel Actuators. *Adv. Sci.* **2019**, *6*, 1801584.

(14) Sutton, A.; Shirman, T.; Timonen, J. V. I.; England, G. T.; Kim, P.; Kolle, M.; Ferrante, T.; Zarzar, L. D.; Strong, E.; Aizenberg, J. Photothermally Triggered Actuation of Hybrid Materials as a New Platform for *in vitro* Cell Manipulation. *Nat. Commun.* **2017**, *8*, 14700.

(15) Huang, W.; Tarakanova, A.; Dinjaski, N.; Wang, Q.; Xia, X.; Chen, Y.; Wong, J. Y.; Buehler, M. J.; Kaplan, D. L. Design of Multistimuli Responsive Hydrogels Using Integrated Modeling and Genetically Engineered Silk-Elastin-Like-Proteins. *Adv. Funct. Mater.* **2016**, *26*, 4113−4123.

(16) Zhou, M. L.; Qian, Z. G.; Chen, L.; Kaplan, D. L.; Xia, X. X. Rationally Designed Redox-Sensitive Protein Hydrogels with Tunable Mechanical Properties. *Biomacromolecules* **2016**, *17*, 3508−3515.

(17) Qian, Z. G.; Zhou, M. L.; Song, W. W.; Xia, X. X. Dual Thermosensitive Hydrogels Assembled from the Conserved C-Terminal Domain of Spider Dragline Silk. *Biomacromolecules* **2015**, *16*, 3704−3711.

(18) Takahashi, R.; Sun, T. L.; Saruwatari, Y.; Kurokawa, T.; King, D. R.; Gong, J. P. Creating Stiff Tough and Functional Hydrogel Composites with Low-Melting-Point Alloys. *Adv. Mater.* **2018**, *30*, 1706885.

(19) Yang, Y.; Wang, X.; Yang, F.; Shen, H.; Wu, D. Universal Soaking Strategy to Convert Composite Hydrogels into Extremely Tough and Rapidly Recoverable Double-Network Hydrogels. *Adv. Mater.* **2016**, *28*, 7178−7184.

(20) Wu, D.; Wang, W.; Diaz-Dussan, D.; Peng, Y. Y.; Chen, Y.; Narain, R.; Hall, D. G. In Situ Forming, Dual-Crosslink Network, Self-Healing Hydrogel Enabled by a Bioorthogonal Nopoldiol−Benzoxaborolate Click Reaction with a Wide pH Range. *Chem. Mater.* **2019**, *31*, 4092−4102.

(21) Azevedo, S.; Costa, A. M. S.; Andersen, A.; Choi, I. S.; Birkedal, H.; Mano, J. F. Bioinspired Ultratough Hydrogel with Fast Recovery, Self-Healing, Injectability and Cytocompatibility. *Adv. Mater.* **2017**, *29*, 1700759.

(22) Cao, J.; Li, J.; Chen, Y.; Zhang, L.; Zhou, J. Dual Physical Crosslinking Strategy to Construct Moldable Hydrogels with

Ultrahigh Strength and Toughness. *Adv. Funct. Mater.* **2018**, *28*, 1800739.

(23) Yang, Y.; Wang, X.; Yang, F.; Wang, L.; Wu, D. Highly Elastic and Ultratough Hybrid Ionic−Covalent Hydrogels with Tunable Structures and Mechanics. *Adv. Mater.* **2018**, *30*, 1707071.

(24) Duan, J.; Liang, X.; Guo, J.; Zhu, K.; Zhang, L. Ultra-Stretchable and Force-Sensitive Hydrogels Reinforced with Chitosan Microspheres Embedded in Polymer Networks. *Adv. Mater.* **2016**, *28*, 8037−8044.

(25) Xia, L. W.; Xie, R.; Ju, X. J.; Wang, W.; Chen, Q.; Chu, L. Y. Nano-Structured Smart Hydrogels with Rapid Response and High Elasticity. *Nat. Commun.* **2013**, *4*, 2226.

(26) Huang, T.; Xu, H.; Jiao, K.; Zhu, L.; Brown, H. R.; Wang, H. A Novel Hydrogel with High Mechanical Strength: a Macromolecular Microsphere Composite Hydrogel. *Adv. Mater.* **2007**, *19*, 1622−1626.

(27) Chen, H.; Yang, F.; Chen, Q.; Zheng, J. A Novel Design of Multi-Mechanoresponsive and Mechanically Strong Hydrogels. *Adv. Mater.* **2017**, *29*, 1606900.

(28) Sun, Z.; Lv, F.; Cao, L.; Liu, L.; Zhang, Y.; Lu, Z. Multistimuli-Responsive, Moldable Supramolecular Hydrogels Cross-Linked by Ultrafast Complexation of Metal Ions and Biopolymers. *Angew. Chem., Int. Ed.* **2015**, *54*, 7944−7948.

(29) George, M.; Abraham, T. E. Polyionic Hydrocolloids for the Intestinal Delivery of Protein Drugs: Alginate and Chitosan - a Review. *J. Controlled Release* **2006**, *114*, 1−14.

(30) Luo, F.; Sun, T. L.; Nakajima, T.; Kurokawa, T.; Zhao, Y.; Sato, K.; Ihsan, A. B.; Li, X.; Guo, H.; Gong, J. P. Oppositely Charged Polyelectrolytes Form Tough, Self-Healing, and Rebuildable Hydrogels. *Adv. Mater.* **2015**, *27*, 2722−2727.

(31) Nisato, G.; Munch, J. P.; Candau, S. J. Swelling, Structure, and Elasticity of Polyampholyte Hydrogels. *Langmuir* **1999**, *15*, 4236−4244.

(32) Sun, T. L.; Kurokawa, T.; Kuroda, S.; Ihsan, A. B.; Akasaki, T.; Sato, K.; Haque, M. A.; Nakajima, T.; Gong, J. P. Physical Hydrogels Composed of Polyampholytes Demonstrate High Toughness and Viscoelasticity. *Nat. Mater.* **2013**, *12*, 932−937.

(33) Roy, C. K.; Guo, H. L.; Sun, T. L.; Ihsan, A. B.; Kurokawa, T.; Takahata, M.; Nonoyama, T.; Nakajima, T.; Gong, J. P. Self-Adjustable Adhesion of Polyampholyte Hydrogels. *Adv. Mater.* **2015**, *27*, 7344−7348.

(34) Baroudi, I.; Simonnet-Jégat, C.; Roch-Marchal, C.; Leclerc-Laronze, N.; Livage, C.; Martineau, C.; Gervais, C.; Cadot, E.; Carn, F.; Fayolle, B.; Steunou, N. Supramolecular Assembly of Gelatin and Inorganic Polyanions: Fine-Tuning the Mechanical Properties of Nanocomposites by Varying Their Composition and Microstructure. *Chem. Mater.* **2015**, *27*, 1452−1464.

(35) Gumerova, N. I.; Rompel, A. Synthesis, Structures and Applications of Electron-Rich Polyoxometalates. *Nat. Rev. Chem.* **2018**, *2*, 0112.

(36) Du, D. Y.; Qin, J. S.; Li, S. L.; Su, Z. M.; Lan, Y. Q. Recent Advances in Porous Polyoxometalate-Based Metal−Organic Framework Materials. *Chem. Soc. Rev.* **2014**, *43*, 4615−4632.

(37) Xu, J.; Li, X.; Li, J.; Li, X.; Li, B.; Wang, Y.; Wu, L.; Li, W. Wet and Functional Adhesives from One-Step Aqueous Self-Assembly of Natural Amino Acids and Polyoxometalates. *Angew. Chem., Int. Ed.* **2017**, *56*, 8731−8735.

(38) Huang, S. C.; Qian, Z. G.; Dan, A. H.; Hu, X.; Zhou, M. L.; Xia, X. X. Rational Design and Hierarchical Assembly of a Genetically Engineered Resilin-Slik Copolymer Results in Stiff Hydrogels. *ACS Biomater. Sci. Eng.* **2017**, *3*, 1576−1585.

(39) Li, J.; Li, X.; Xu, J.; Wang, Y.; Wu, L.; Wang, Y.; Wang, L.; Lee, M.; Li, W. Engineering the Ionic Self-Assembly of Polyoxometalates and Facial-Like Peptides. *Chem. - Eur. J.* **2016**, *22*, 15751−15759.

(40) Xu, J.; Li, X.; Li, X.; Li, B.; Wu, L.; Li, W.; Xie, X.; Xue, R. Supramolecular Copolymerization of Short Peptides and Polyoxometalates: Toward the Fabrication of Underwater Adhesives. *Biomacromolecules* **2017**, *18*, 3524−3530.

(41) Berth, G.; Dautzenberg, H.; Peter, M. G. Physico-Chemical Characterization of Chitosans Varying in Degree of Acetylation. *Carbohydr. Polym.* **1998**, *36*, 205−216.

(42) Jürgensen, A.; Moffat, J. B. The Stability of 12-Molybdosilicic, 12-Tungstosilicic, 12-Molybdophosphoric and 12-Tungstophosphoric Acids in Aqueous Solution at Various pH. *Catal. Lett.* **1995**, *34*, 237−244.

(43) Wang, S. M.; Hwang, J.; Kim, E. Polyoxometalates as Promising Materials for Electrochromic Devices. *J. Mater. Chem. C* **2019**, *7*, 7828−7850.

(44) Zhang, Y. S.; Khademhosseini, A. Advances in Engineering Hydrogels. *Science* **2017**, *356*, eaaf3627.

(45) Bijelic, A.; Aureliano, M.; Rompel, A. Polyoxometalates as Potential Next-Generation Metallodrugs in the Combat Against Cancer. *Angew. Chem., Int. Ed.* **2019**, *58*, 2980−2999.